Effect of Etherification Reaction on Extraction and Photoelastic and Dynamic Mechanical Behavior of Diepoxide–Diamine Networks

A. VAZQUEZ,[1] M. ILAVSKÝ,[2,3] K. DUŠEK[2]

[1] Institute of Materials Science and Technology, University of Mar del Plata and National Research Council, J.B. Justo 4302, Mar del Plata, Argentina

[2] Institute of Macromolecular Chemistry, Academy of Sciences of the Czech Republic, 162 06 Prague 6, Czech Republic

[3] Faculty of Mathematics and Physics, Charles University, 180 00 Prague 8, Czech Republic

Received 3 November 1998; accepted 15 April 1999

ABSTRACT: Sol fraction and equilibrium photoelastic and dynamic mechanical behavior of epoxide networks based on bisphenol A diglycidyl ether (DGEBA) and poly(oxypropylene diamine) (Jeffamine® D-400) with four initial molar ratios of epoxy (E) and amine (A) groups, $r_E = [E]_0/(2[A]_0) = 1.2$, 1.5, 2.0, and 2.3 were investigated. Networks with different extents of total epoxy group conversions (including etherification), α_E, were prepared for each r_E value. Both the ratio r_E and the conversion α_E affected the value of the equilibrium modulus, G, and the weight fraction of the gel, w_g. As expected, decreasing the r_E ratio (at constant α_E) and increasing α_E (at constant r_E) were accompanied by an increase in the modulus, G, and gel fraction, w_g. The stress optical coefficient, C, is independent of α_E decreasing with increasing r_E. The frequency–temperature superposition could be performed for all networks; the temperature dependence of the horizontal shift factor, a_{To}, satisfied the WLF equation. The temperature and time positions of viscoelastic functions predominantly depend on the overall concentration of elastically active network chains ν_e, regardless of the values of r_E and α_E. While the shape of viscoelastic functions at the beginning of the main transition region depended on the detailed structure of the chain (number and length of pendant chains), the shape at the end of the transition was determined mainly by the concentration of elastically active network chains. An unexpected universal increase was found in the half-width of the maximum in the dependence of the superimposed loss compliance, J''_p, on reduced frequency ωa_T with increasing crosslinking density. © 1999 John Wiley & Sons, Inc. J Appl Polym Sci 74: 2877–2885, 1999

Key words: polyetherification; photoelasticity; sol fraction; epoxide networks; viscoelasticity

INTRODUCTION

Mechanical properties of crosslinked epoxide resins have been widely studied.[1–8] Simple crosslinked epoxide–amine systems have also been used for testing of network formation and rubber elasticity theories.[3,5,9,10] Flexible epoxide–amine networks were prepared from diglycidyl ether of bisphenol A (DGEBA) and poly(oxypropylene diamine) or -triamine) (Jeffamine).[11a,11b] Also some off-stoichiometric networks from DGEBA and 4,4′-diaminodiphenylmethane (DDM) are flexible

Correspondence to: M. Ilavský.

Journal of Applied Polymer Science, Vol. 74, 2877–2885 (1999)
 CCC 0021-8995/99/122877-09

at room or somewhat elevated temperature.[4,9,10] The buildup process and network structure prepared with amine groups in excess can be described by the theory of branching processes if the difference in reactivities of primary and secondary amino groups is taken into account.[3–5] It has been found[5,8,11] that the frequency and temperature positions of viscoelastic mechanical functions predominantly depend on crosslinking density. The shape of dynamic mechanical functions is dependent on the structure of elastically active network chains (EANCs),[11] particularly on whether the EANCs are smooth or have dangling chains. These conclusions follow from the studies of the poly(oxypropylene diamine)–DGEBA system prepared with an excess of amine groups.[11]

Stoichiometric epoxide–amine networks and networks with excess amino groups at complete reaction of epoxide groups do not undergo any further reaction, at least below 180°C. If epoxide groups are in excess, etherification by the ring-opening reaction induced by the OH groups of the formed amino alcohol can interfere.[2,11–17,18a] Crosslinking by etherification is also important in practice. The reaction mechanism of the epoxide–amine addition and subsequent etherification was originally considered as an initiated stepwise polyaddition in which the OH group was reformed in each step. However, the mechanism has been found to be much more complex (see for example Ref. 16); the addition of epoxide groups proceeds by several paths; the control by chain transfer accompanied by reinitiation is the most important. As a result, the polyether sequences are rather short.

For aliphatic and aromatic polyamines, the amine–epoxide reaction is, as a rule, much faster than etherification released by aminoalcohols. This is manifested by both primary amine hydrogens reacting first and completely; only then does etherification start.[18c] However, in the case of poly(ether amine)s the situation is different: (1) the reactivity of amino end groups in the reaction with epoxide groups is lower in comparison with that of aliphatic and aromatic amines due to the presence of donor–acceptor ether groups of the poly(oxypropylene)[19]; (2) also the substitution effect in the amino group expressed by the ratio of reactivity of secondary amino groups to that of primary amino groups is more negative. As a result, etherification starts before all amine hydrogens have reacted.

In our previous paper,[11] we studied mechanical behavior of epoxide networks prepared from poly(oxypropylene diamine) and DGEBA with an excess of amino groups; the conversion of epoxide groups in these networks was almost complete. This contribution is focused on systems in which epoxide groups are in excess, and ether bonds are formed in addition to C—N bonds in the reaction of epoxide with amine. The effect of etherification on sol fraction and equilibrium and dynamic mechanical as well as photoelastic behavior is examined.

MATERIALS AND METHODS

Sample preparation: The networks were prepared from diglycidyl ether of bisphenol A (DGEBA, epoxy equivalent $\gamma_E = 175.4$ g/mol epoxy, number-average molar mass $M_n = 350$ g/mol, number-average functionality $f_n = 2$) and poly(oxypropylene diamine) (Jeffamine® D-400, $\gamma_A = 106.4$ g/mol H, $M_n = 370$ g/mol, $f_n = 3.75$). Four series of networks were prepared with various constant ratios of the initial epoxide (E) and amino (NH_2) groups, $r_E = [E]_0/(2[NH_2]_0) = 1.2$, 1.5, 2.0, and 2.3, and with varying extents of total epoxy groups conversion, α_E (Table I). The curing proceeded at $T_c = 150$°C for various reaction times, t_c, in the range 0 to 50 days in $10 \times 10 \times 0.1$ cm^3 hydrophobized glass molds. The procedures used in the purification and characterization of starting compounds have been described earlier.[19]

The overall conversion of epoxide groups, α_E, is given by

$$\alpha_E = ([E]_0 - [E])/[E]_0 \quad (1)$$

where $[E]_0$ and $[E]$ are initial and actual concentrations of epoxide groups, respectively. The concentration of unreacted epoxide groups, $[E]$, was determined by near-infrared spectrometry using the band at 4,530 cm^{-1} (the molar absorption coefficient, $\varepsilon = 1.2$, is independent of the concentration of epoxide groups[20]).

Photoelastic measurements: Photoelastic characteristics were measured with the earlier-described apparatus,[21] in which both the force relaxation, $f(t)$, and the optical retardation relaxation, $\delta(t)$ (and thus also the birefringence relaxation, $\Delta n(t) = \lambda_0 \delta(t)/2$, where d is the deformed thickness of the sample, and $\lambda_0 = 546.1$ nm is the wavelength of the light), could be re-

Table I Extraction, Equilibrium Photoelastic, and Dynamic Mechanical Characteristics

α_E	w_s	G MPa	$C \times 10^4$ MPa^{-1}	T_m °C	c_1^{65}	c_2^{65} °C	log G''_m MPa	h^1 °C	log J''_m MPa^{-1}	log h^2 (rad s^{-1})	log ω_r (rad s^{-1})
						$r_E = 1.2$					
0.876	0.042	1.92	19.7	35	8.68	79.8	2.22	11.2	−0.96	1.6	2.0
0.921	0.028	2.81	19.2	38	11.20	78.6	2.16	11.0	−0.96	1.8	1.8
0.954	0.021	3.04	19.1	47	11.18	68.1	2.15	11.0	−1.10	1.7	1.2
0.955	0.020	3.25	19.2	—	—	—	—	—	—	—	—
0.986	0.011	4.04	19.8	51	10.83	64.8	2.11	11.2	−1.24	2.1	0.6
						$r_E = 1.5$					
0.710	0.156	0.68	18.0	25	7.75	63.1	2.30	12.0	0.55	1.7	1.8
0.733	0.137	1.03	18.2	—	—	—	—	—	—	—	—
0.825	0.074	2.17	18.4	38	10.60	78.2	2.20	12.4	0.70	1.9	1.5
0.845	0.064	2.48	19.6	44	10.50	71.6	2.19	13.2	−1.08	2.0	1.2
0.916	0.047	3.84	18.9	52	11.13	93.9	2.14	13.4	−1.20	2.2	0.0
1.000	0.040	4.20	18.6	—	—	—	—	—	—	—	—
						$r_E = 2.0$					
0.530	0.570	0.04	17.7	16	7.69	102.7	2.34	10.0	0.10	0.8	3.6
0.591	0.482	0.14	17.0	17	6.44	100.4	2.30	12.0	−0.02	1.3	3.1
0.680	0.260	0.79	16.4	26	7.32	91.6	2.27	13.6	−0.84	1.7	2.0
0.707	0.200	1.27	17.5	32	8.27	83.4	2.25	13.6	−1.00	2.0	−0.2
0.819	0.130	2.53	18.2	50	9.98	66.6	2.16	15.5	−1.10	2.2	−0.8
0.913	0.060	4.09	17.8	60	10.24	67.6	2.13	17.2	−1.20	2.3	−1.6
0.972	0.057	3.83	16.9	65	10.80	65.0	2.10	17.8	−1.36	2.4	−1.7
1.000	0.050	4.17	18.8	—	—	—	—	—	—	—	—
						$r_E = 2.3$					
0.613	0.214	0.51	15.9	24	8.46	91.7	8.25	15.2	0.70	1.4	2.65
0.698	0.120	1.66	15.5	35	8.97	76.9	8.23	17.0	−1.20	1.6	1.30
0.862	0.052	4.20	16.5	57	13.09	61.2	8.11	18.2	−1.30	2.0	−1.50
0.980	0.065	5.20	16.0	—	—	—	—	—	—	—	—

corded. The measurements were performed with dry, unextracted rectangular samples ($5 \times 1 \times 0.1$ cm^3) at temperature $T = 107$°C in nitrogen atmosphere. Strain dependence of stress, $\sigma = f/A$ (where A is the deformed cross section of the sample) and of birefringence Δn at various elongations Λ ($1 < \Lambda < 1.1$, usually 10 Λ values) after 60 s of relaxation at each Λ were determined. This time was sufficient for the achievement of equilibrium force value for all samples. From these measurements, the initial modulus, G, the deformation–optical function, A, and the stress–optical coefficient, $C = A/G$, were determined using the following relations[21,22]:

$$\sigma = G(\Lambda^2 - \Lambda^{-1}) \tag{2}$$

$$\Delta n = A(\Lambda^2 - \Lambda^{-1}) \tag{3}$$

Dynamic mechanical measurements: The dynamic mechanical behavior was characterized using a Rheometrics SYS-4 apparatus on rectangular samples ($5 \times 1 \times 0.1$ cm^3) in a nitrogen atmosphere. The real, G', and imaginary, G'', components of the complex shear modulus, G^* ($=G' + iG''$) or real, J', and imaginary, J'', components of the complex shear compliance, J^* ($=J' - iJ''$) and of the loss tangent, $tg\ \delta$ ($=G''/G' = J''/J'$), were determined in the temperature interval between −50 and 100°C and at the angular rate, ω, which varied from 10^{-2} to 10^2 rad/s. From the temperature dependence of the loss modulus, G'', measured at frequency $f = \omega/2\pi = 1$ Hz, the temperature of the maximum, T_m, the height of the maximum, G''_m, and half-width of the maximum (width in °C at the half-height of the maximum), h^1, were determined.

Using the frequency–temperature superposition, the superimposed curves of both components of the modulus, $G'_p = G'b_T$ and $G''_p = G''b_T$, or compliance, $J'_p = J'/b_T$ and $J''_p = J''/b_T$, were obtained in dependence on reduced angular rate,

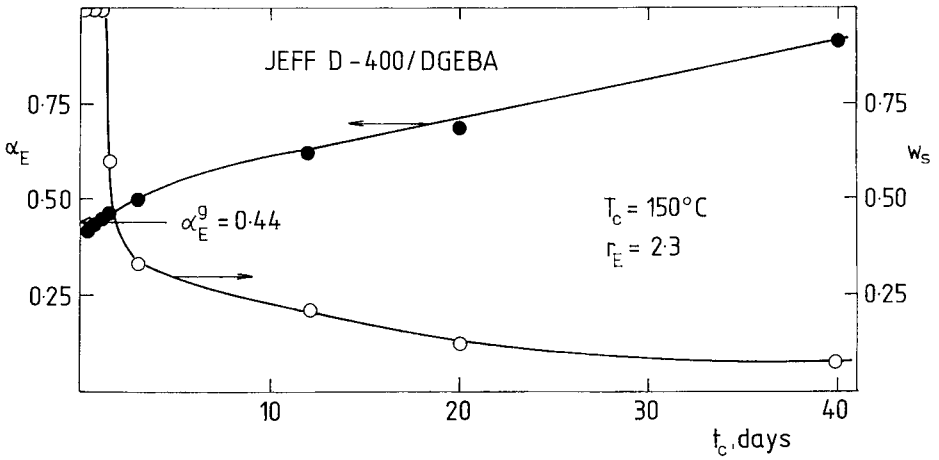

Figure 1 A measured dependence of the conversion of epoxide groups, α_E, and sol fraction, w_s, on the curing time t_c for $r_E = 2$ (α_E^g denotes the gel point conversion).

ωa_{To}, shifted to reference temperature $T_0 = 65°C$ of individual networks. The horizontal shift factor, a_T, was obtained mainly from the superposition of the loss angle tangent $tg\,\delta$ (since no vertical shift for loss angle tangent is necessary, $tg\,\delta_p = tg\,\delta$), and vertical shift b_T was derived mainly from superposition of loss compliance J''.

Extraction of networks: The networks were extracted with a large excess of dioxane. After repeated extraction, the samples were dried in a vacuum box at 50°C to constant weight. The weight fractions of sol, w_s, and gel, $w_g = 1 - w_s$, were determined from the weight of samples before and after the extraction (Table I).

RESULTS AND DISCUSSION

Sol Fraction and Equilibrium Behavior

An example of the observed increase in the conversion of epoxy groups, α_E, and the decrease in the sol fraction, w_s, with curing time, t_c, is shown in Figure 1 for ratio $r_E = 2.3$. Although for short times, $t_c \leq 30$ h, the system is soluble, for longer times, the insoluble gel fraction $w_g = 1 - w_s$ can be found. As expected, with increasing t_c, both α_E and w_g values increase. It is interesting to note that at full conversion of epoxy groups, ~ 5 wt % of the sol is still present in the network. From Figure 1, the gel point conversion, $\alpha_E^g = 0.44$, could also be determined. For the other three series, the values $\alpha_E^g = 0.8$, 0.64, and 0.52 were found for $r_E = 1.2$, 1.5, and 2, respectively. It is also of interest that the theoretical values, $(\alpha_E^g)_t = 0.39$, 0.42, 0.49, and 0.56, are predicted for $r_E = 2.3$, 2, 1.5, and 1.2, respectively, using the theory proposed earlier,[18b] with consideration of the substitution effect in amino group (reactivity

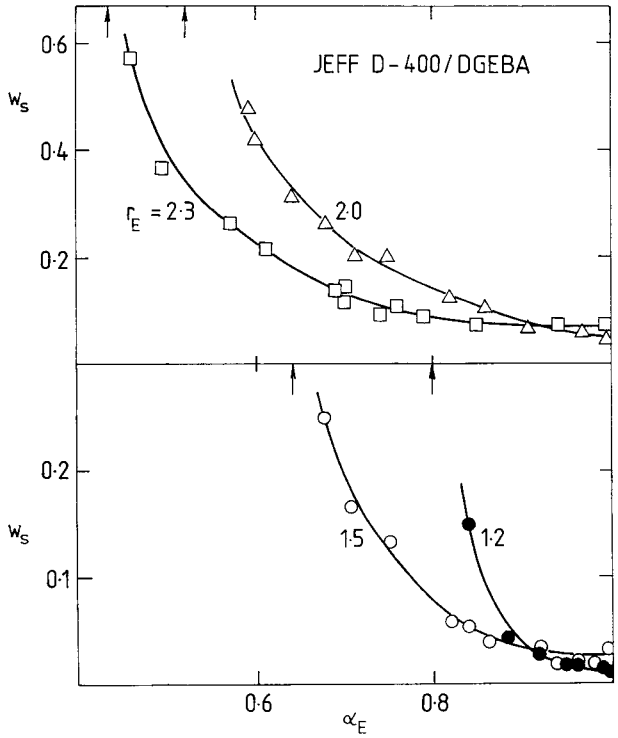

Figure 2 Dependence of the weight fraction of sol, w_s, on the conversion of epoxide groups, α_E, for samples of different r_E values (the arrows show the gel point conversions).

ratios of hydrogens in primary and secondary amino groups, $k_2/2k_1 = 0.2$). As α_E^g values are always higher than $(\alpha_E^g)_t$ values, chain transfer reactions accompanied by reinitiation control the etherification from the beginning.

As expected, with increasing epoxy groups conversion, α_E, the sol content, w_s, decreases for all network series (Figure 2). In all network series, for $\alpha_E \rightarrow 1$, nonzero values of sol fractions were found (Table I). Such an unusual finding is in agreement with the complex reaction mechanism of the etherification reaction.[16]

With increasing α_E, the moduli values G of individual series increase (Table I). The difference between curves for different r_E at constant $\alpha_E \rightarrow 1$ is not large since α_E is a measure of the number of bonds per epoxide unit. The stress–optical coefficient C is practically independent of α_E in individual network series (Table I). On the other hand, C decreases with increasing excess of epoxy component, which suggests a higher positive contribution of Jeffamine® D-400 to birefringence as compared with the contribution of DGEBA. Similar results were found for epoxy networks based on DGEBA and 4,4′-diaminodiphenylmethane.[4]

Assuming that the sol and gel densities are the same and that sol acts as a diluent for the network, it is possible, from the values of the moduli G, to calculate the experimental concentration of elastically active network chains (EANCs), ν_e, as-

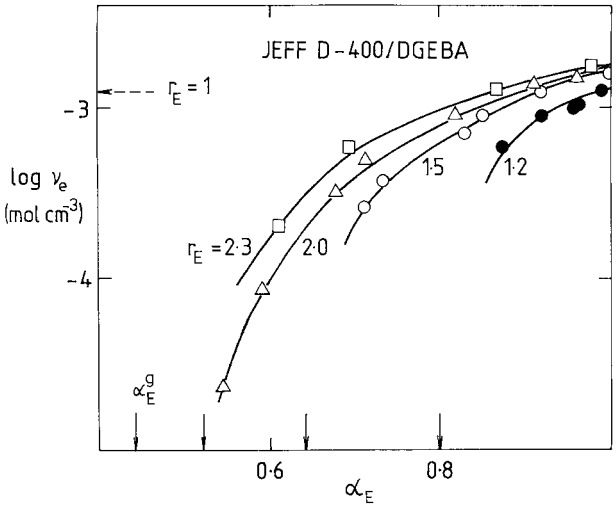

Figure 3 Dependence of the concentration of elastically active network chains, ν_e, on the conversion of epoxide groups, α_E. (The gel point conversions, α_E^g, are shown by arrows at the α_E axis; — > denotes the ν_e value for a fully cured stoichiometric network with $r_E = 1$.)

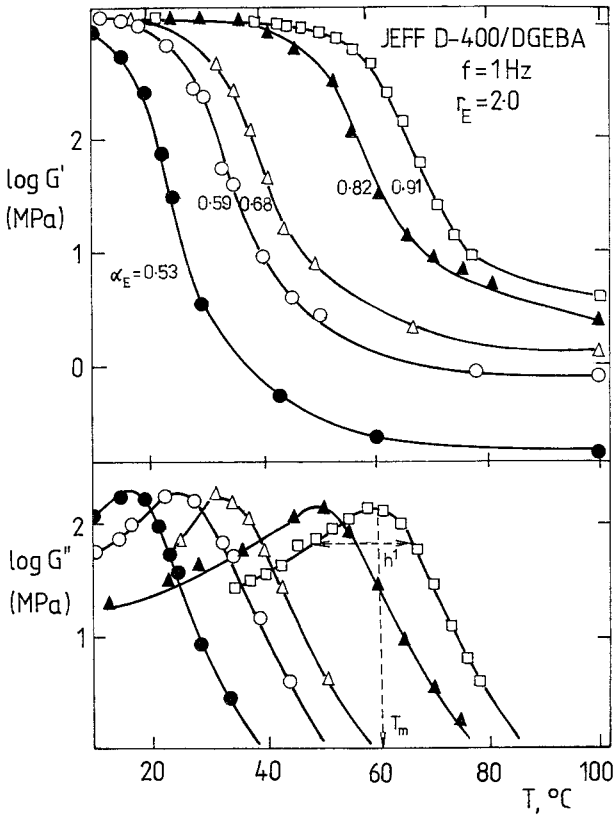

Figure 4 An example of measured temperature dependences of the real, G', and the loss, G'', moduli for networks with $r_E = 2$.

suming the validity of the constrained junction model

$$\nu_e = G/(w_g RT) \tag{4}$$

where R is the gas constant and the temperature of measurement $T = 380$ K. Figure 3 shows the dependence of ν_e on α_E for individual network series. It is interesting to note that in the region $\alpha_E > 0.95$, the ν_e values of all series approach the value for the fully cured stoichiometric Jeffamine D-400–DGEBA network[11] with $r_E = 1$ ($\nu_e = 1.5 \times 10^{-3}$ mol cm^{-3}).

Dynamic Mechanical Behavior

Temperature Dependences

An example of the effect of the extent of epoxy reaction on the temperature dependence of the storage, G', and the loss, G'', moduli (measured at 1 Hz) of samples with $r_E = 2$ is given in Figure 4. With increasing α_E, both components of the modulus are shifted to higher temperatures. The

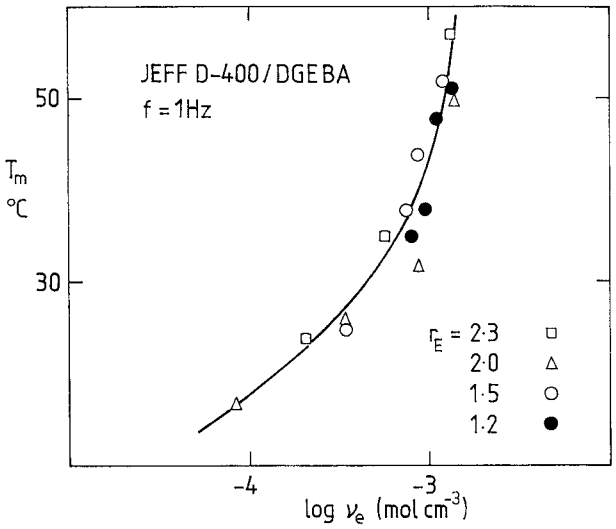

Figure 5 Dependence of the temperature of the maxima, T_m, (from the dependence of G'' on T) on the EANC concentration, ν_e.

shape of the log G' versus T dependence in the main transition region varies little; in accord with this finding, only a small increase in the half-width h_1 (determined from the dependence of log G'' on T, Fig. 4, Table I) with increasing α_E was found. As expected, the G' values in the rubber-like region increase quickly with increasing α_E, thus indicating an increase in the concentration of EANCs, ν_e, in the system. Similar results were obtained for three other network series with constant ratios r_E = 1.2, 1.5, and 2.3.

With an increasing extent of epoxy reaction, the T_m values (T_m is the maximum temperature of the $G'' - T$ dependence, which corresponds to the glass transition temperature $T_m \cong T_g$ + 10–15°C, Fig. 4) increase in the individual network series (Table I). From Figure 5, in which the dependence of T_m on the concentration of EANCs, ν_e, is shown, it can be seen that an universal dependence of T_m on ν_e for all networks is found. This result means that the temperature position of the main transition region is predominantly affected by the concentration of EANCs irrespective of the composition ratio r_E and the extent of etherification.

The temperature dependences of the horizontal shift factors, log a_T, of all networks are adequately described by the WLF equation[23]

$$\log a_{T_0}(T) = -c_1^0(T - T_0)/(c_2^0 + T - T_0) \quad (5)$$

where T_0 = 65°C is the reference temperature (Table I). From the constants c_1^0 and c_2^0, the free-volume characteristics, the fractional free volume $f^0 (= 1/(2.3\ c_1^0)$ and the thermal expansion coefficient of the free volume $\alpha_f (= 1/(2.3\ c_1^0 c_2^0))$, were calculated (Fig. 6). While the α_f values vary within the experimental error and are independent of ν_e, the fractional free volumes f^0 decrease with increasing EANC concentration. The decrease in f^0 is mainly due to the observed shift of the main transition region to higher temperatures with increasing ν_e (see Figs. 4 and 5); the calculated value of fractional free volume at T_m, f^m is practically constant ($f^m \cong 0.03$) for all samples (Fig. 6). Since T_m is related to the glass transition temperature, it can be expected that the fractional free volume at T_g, f^g, would be lower by ~ 20% than f^m (α_f values remain unaffected) and approach the universal value[23] ($f^g \approx 0.025$).

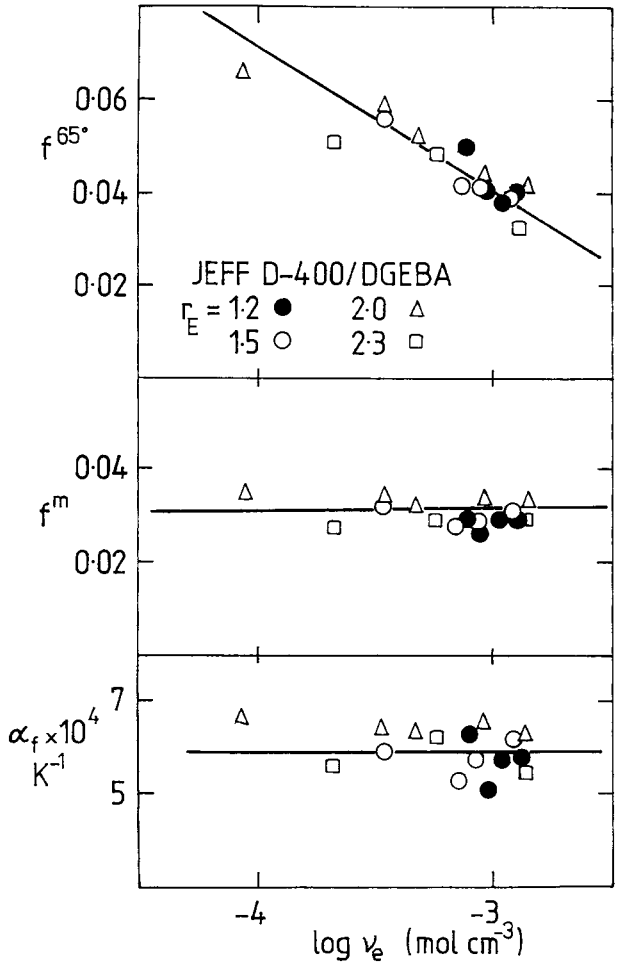

Figure 6 Dependence of the fractional free volumes, f^m, and f^{65}, and of the coefficient of temperature expansion of the free volume, α_f, on the EANC concentration, ν_e.

Frequency Dependences

The dependences of superimposed curves of the loss compliance J''_p for $T_0 = 65°C$ are shown in Figures 7 and 8. In each series of networks, with increasing α_E, the loss curves J''_p are shifted to lower frequencies. Close to the rubbery region (low frequencies, Fig. 7), the dependences of J''_p on reduced frequency ωa_T pass through a maximum for which the height J''_m, its frequency position ω_m and the half-width h^2 were determined (Table I, Fig. 7). From Figures 7 and 8 it follows that with increasing α_E, the height of the maximum of the loss compliance J''_m decreases and the half-width h^2 increases. As the crosslinking density in the system increases with increasing α_E (increasing extent of the etherification reaction), this is an unusual observation. In most network systems, opposite dependences are usually found; for example, an increase in h^2 was observed[11,23,24] with decreasing EANC concentration as the length and complexity of the chain between the crosslinks increases with decreasing ν_e.

An unexpected increase in both half-widths, h^1 (obtained from maximum of G'' on temperature) and h^2 (from maximum of J''_p on ωa_{T_0}) with increasing EANC concentration, ν_e, is shown in Figure 9. The practically universal dependence of h^2 on ν_e reveals that the shape of viscoelastic functions at the end of the main transition region is determined mainly by the concentration of EANCs. On the other hand, the varying dependences of h^1 on ν_e for individual series prepared at various constant r_E suggest that the shape of mechanical functions at the beginning of the main transition depends on the detailed structure of the EANC chain; networks with the highest r_E values also showed the largest h^1 values at constant ν_e. We believe that a decisive role in increasing h^1 value with r_E is played by the number and length of pendant chains. An unexpected increase in the half-widths h^1 and h^2 with increasing ν_e was observed earlier[8] for networks prepared from *N,N,N′,N′*-tetraglycidyl-4,4′-diaminodiphenylmethane (TGDDM) and DDM. Similar to previous papers,[8,25] we believe that the stiffness of the chain increases with increasing ν_e, which leads to a broadening of the free volume distribution function and to an increase in the half-widths with ν_e.

With increasing EANC concentration, ν_e, the height of the maximum J''_m (and thus[23] also the

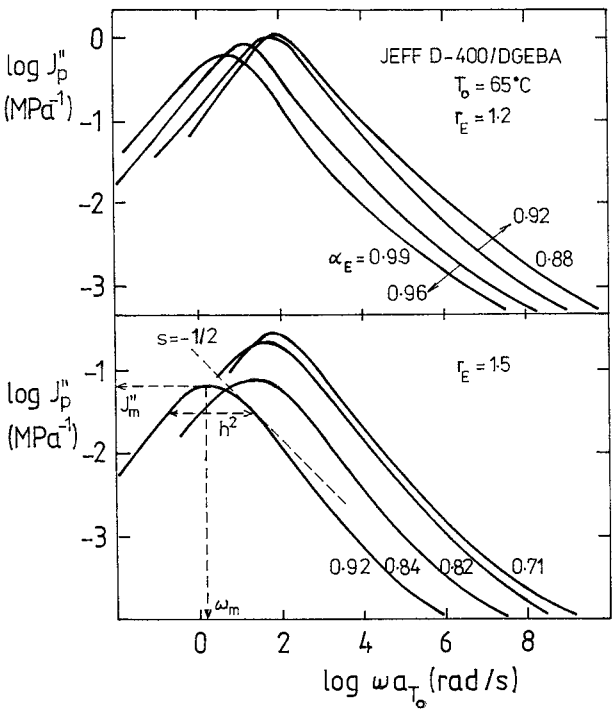

Figure 7 Dependence of the superimposed reduced-loss compliances, log J''_p, on the reduced frequency, log ωa_T, for networks with $r_E = 1.2$ and 1.5.

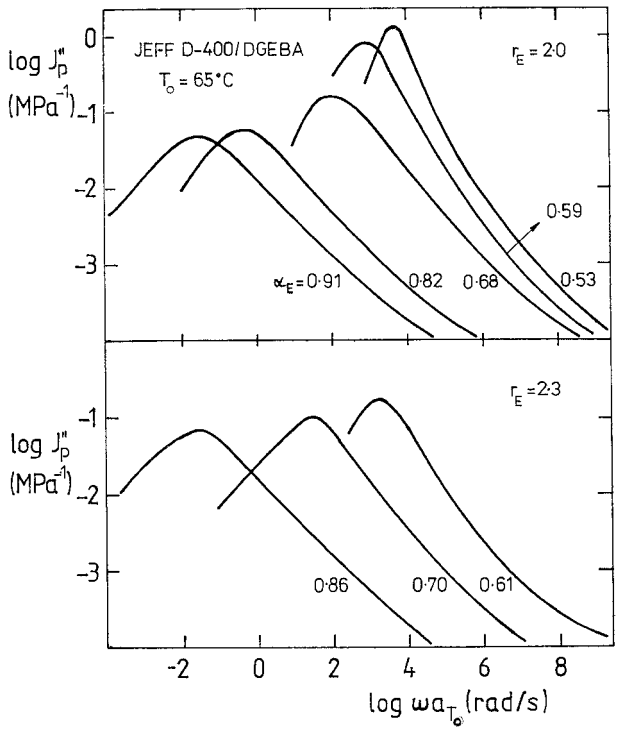

Figure 8 Dependence of the superimposed reduced-loss compliances, log J''_p, on the reduced frequency, log ωa_T, for networks with $r_E = 2$ and 2.3.

height of retardation spectrum $L_m = (2/\pi)J''_m$) decreases (Fig. 10). The observed decrease is the same for all samples, which suggests a decisive effect of crosslinking density on the J''_m value. It is interesting to note that the product $J''_m G$ is roughly constant (changing from 0.1 to 0.25) and independent of the composition r_E and the extent of epoxy conversion α_E. Various molecular theories of polymer networks[23,24] predict a constant value of $J''_m G$ (or $L_m G$), which can vary from 0.26 to 0.42 in dependence on the distribution of submolecules in the chain (the broader the distribution, the lower the $J''_m G$ product). As expected, the increasing crosslinking density shifts the maximum of J'' to lower frequencies, ω_m at constant temperature (Fig. 10, Table I). The dependence of ω_m on ν_e is also independent of r_E and α_E (Fig. 10).

The authors thank the grant agency of Charles University for support under Grant No. FYZ 46/1998 B and the grant agency of the Academy of Sciences of the Czech Republic (Grant No. A4050808).

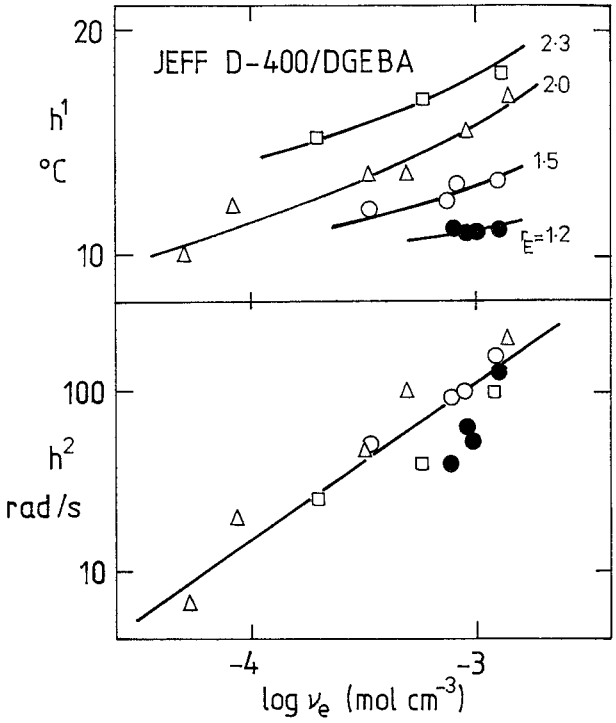

Figure 9 Dependence of the half-width h^1 (from the dependence of G'' on T) and of the half-width h^2 (from the dependence of J''_p on ωa_T) on the EANC concentration, ν_e.

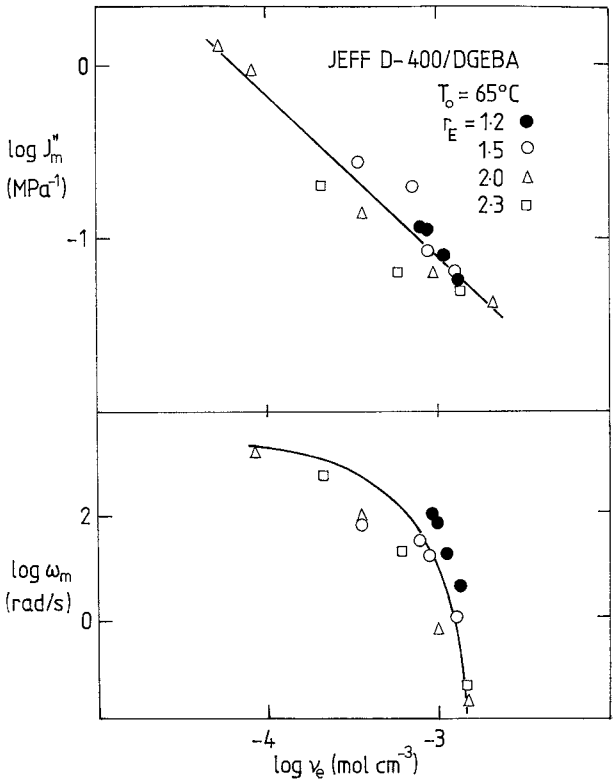

Figure 10 Dependence of the loss maximum, J''_m, and its frequency position, ω_m, on the EANC concentration, ν_e.

REFERENCES

1. Epoxy Resins. Chemistry and Technology. May, C. A.; Dekker, M., Eds.; New York, 1988.
2. Morgan, R. J. Adv Polym Sci 1985, 72, 1.
3. Dušek, K. Adv Polym Sci 1986, 78, 1.
4. Ilavský, M.; Bogdanova, L. M.; Dušek, K. J Polym Sci, Polym Phys Ed 1984, 22, 265.
5. Ilavský, M.; Hrouz, J. J Non-Cryst Solids 1991, 131, 906.
6. Vakil, U. M.; Martin, G. C. J Appl Polym Sci 1992, 46, 2089.
7. Grillet, A. C.; Galy, J.; Gerard, J.-F.; Pascault, J.-P. Polymer 1991, 32, 1885.
8. Ilavský, M.; Dušek, K.; Zelenka, J.; Dobáš, I. Polym Networks Blends 1995, 4, 187.
9. Dušek, K.; Ilavský, M.; Luňák, S. J Polym Sci, Polym Symp 1975, 53, 29.
10. Dušek, K.; Ilavský, M. J Polym Sci, Polym Phys Ed 1983, 21, 1323.
11. Ilavský, M.; Hrouz, J.; Šomvársky, J.; Dušek, K. Makromol Chem, Macromol Symp 1989, 30, 13.
12. Rozenberg, B. A. Adv Polym Ser 1985, 75, 113.
13. Berger, J.; Lohse, F. Eur Polym J 1985, 21, 435.

14. Riccardi, C. C.; Williams, R. J. J. Polymer 1986, 27, 913.
15. Dušek, K. Polym Bull 1985, 13, 321.
16. Vazquez, A.; Matějka, L.; Špaček, P.; Dušek, K. J Polym Sci, Polym Chem Ed 1990, 28, 2305.
17. Dušek, K.; Šomvársky, J.; Ilavský, M.; Matějka, L. Comput Polym Sci 1991, 1, 90.
18. (a) Zukas, W. X.; Schneider, N. S.; MacKnight, W. J. Polym Mater Sci Eng 1983, 49, 588. (b) Dušek, K.; Ilavský, M.; Šomvársky, J. Polym Bull 1987, 18, 209. (c) Morgan, J. R.; Mones, E. T. J Appl Polym Sci 1987, 33, 999. (d) Fryhauf, K.; Strehmel, V.; Fedtke, M. Polymer 1993, 34, 327. (e) Zukas, W. X. Polym Mater Sci Eng 1996, 75, 123. (f) Xu, L.; Schlup, J. R. J Appl Polym Sci 1998, 67, 895.
19. Dušek, K.; Ilavský, M.; Štokrová, Š.; Matějka, L.; Luňák, S. In Crosslinked Epoxies; Sedláček, B.; Kahovec, J., Eds.; Walter de Gruyter: Berlin, 1987, p 269.
20. Zelenka, J.; Ilavský, M.; Špaček, V.; Štokrová, Š.; Klaban, J.; Dušek, K. Colloid Polym Sci 1991, 269, 1013.
21. Ilavský, M.; Dušek, K. Collect Czech Chem Commun 1977, 42, 1152.
22. Treloar, L. R. G. The Physics of Rubber Elasticity, Oxford, 1975.
23. Ferry, J. D. Viscoelastic Properties of Polymers, 2nd ed.; Interscience: New York, 1970.
24. Ilavský, M.; Hasa, J. J Polym Sci, Polym Phys Ed 1970, 11, 539.
25. Mason, P. Polymer 1964, 5, 625.